10

GALVANIC CORROSION

X. G. ZHANG
Teck Metals Ltd., Mississauga, Ontario, Canada

A. INTRODUCTION

Galvanic corrosion, resulting from a metal contacting another conducting material in a corrosive medium, is one of the most common types of corrosion. It may be found at the junction of a water main, where a copper pipe meets a steel pipe, or in a microelectronic device, where different metals and semiconductors are placed together, or in a metal matrix composite material in which reinforcing materials, such as graphite, are dispersed in a metal, or on a ship, where the various components immersed in water are made of different metal alloys. In many cases, galvanic corrosion may result in quick deterioration of the metals but, in other cases, the galvanic corrosion of one metal may result in the corrosion protection of an attached metal, which is the basis of cathodic protection by sacrificial anodes.

Galvanic corrosion is an extensively investigated subject, as shown in Table 10.1, and is qualitatively well understood but, due to its highly complex nature, it has been difficult to deal with in a quantitative way until recently. The widespread use of computers and the development of software have made great advances in understanding and predicting galvanic corrosion.

B. DEFINITION

When two dissimilar conducting materials in electrical contact with each other are exposed to an electrolyte, a current, called the galvanic current, flows from one to the other. Galvanic corrosion is that part of the corrosion that occurs at the anodic member of such a couple and is directly related to the galvanic current by Faraday's law.

Under a coupling condition, the simultaneous additional corrosion taking place on the anode of the couple is called the local corrosion. The local corrosion may or may not equal the corrosion, called the normal corrosion, taking place when the two metals are not electrically connected. The difference between the local and the normal corrosion is called the difference effect, which may be positive or negative. A galvanic current generally causes a reduction in the total corrosion rate of the cathodic member of the couple. In this case, the cathodic member is cathodically protected.

Uhlig's Corrosion Handbook, Third Edition, Edited by R. Winston Revie

TABLE 10.1. Studies on Galvanic Actions of Miscellaneous Alloys In Various Environments

Alloy 1	Alloy 2	Measurements[a]	Focus	References
		Atmosphere		
Steel, S. steel	Al	Weight loss	Automotive parts	1
Al, Cu, Pb, Sn, Mg, Ni, Zn, steel, S. steel	Miscellaneous	Weight loss	Corrosion rate	2
Pt	Zn	I_g	Humidity sensor	3
Al, Cu alloys, Ni, Pb, Zn, steel, S. steels	Miscellaneous	Weight loss	Tropical data	4
Cu	Steel	I_g, weight loss	Corrosion probe	5
Al alloys	S. steel	E_{corr}, I_g	Inhibitors	6
Al, Cu alloys, Ni, Pb, S. steels	Miscellaneous	Weight loss	Clad metals	7
		Fresh Water (pure, river, lake, and underground)		
Co alloys	Carbon	*E–I* curves	Magnetic disc	8
Cu	Ag	E^{d}_{corr}	Electrical contact	9
Steel	Zn	E_g, I_g	Polarity reversal	10, 11
Steel	Zn	E_g, I_g	Polarity reversal	12, 13
Al, Cu alloys, Ni, Pb, Zn, steel, S. steels	Miscellaneous	Weight loss	Damage data	14
Al	Steel	E_{corr}, E_g	Polarity reversal	15
		Seawater		
S. steel	Steel	Thickness loss	Metallic joints	16
S. steel, Ti	Brass, bronze	I_g	Corrosion rate	17
S. steel	Cu	*E–I* curves, E_{corr}	Localized corrosion	18
Steel	Zn	E_g	Transient *E–t*	19
Cu alloys	Cu alloys	Weight loss	Effect of sulfide	20
Miscellaneous	Miscellaneous	E_{corr}, *E–I* curves	Review	21
Al, Cu alloys, Ni, Pb, Zn, steel, S. steels	Miscellaneous	Weight loss	Damage data	14
Steels, S. steels, Cu alloys	Ti alloys, S. steel	I_g, E_c,	Power plant condenser	22
Cu–Ni, Ti	Bronze, Zn	*E* distribution	Cathodic protection	23
Al alloys	S. steel	E_{corr}, I_g	Inhibitors	6
S. steel	Ni alloys, graphite	Miscellaneous	Review	24
Bronze, Ti,	Cu–Ni, Zn, bronze	*E–I* curves	Time effect	25
Cu alloy, Fe, Zn, S. steel	Miscellaneous	E_g, I_g, E_{corr}	Materials interaction	26
		Soils		
Brass, steel	Brass, Pb, Cu, Zn	Weight loss	Corr. and protection	27
S. steel	Zn	I_g	Soil resistance	28
Steel, Zn, Pb	Pb, Cu, steel	IR drop	E_c–E_a	29
		Acids		
S. steels, Ti	Ni alloys	I_g, E_g, *E–I*, weight loss	Prediction	30
Ni alloys	Ni alloys	Thickness loss	Welds	31
Fe–Cr–Ni alloys	Austenite/ferrite	Weight loss, morphology	Phase interaction	32
Fe–Ni, Ti, S. steel, Ni alloys	Graphite, Ni alloys	I_g, E_g, *E–I* curves	Polarization effects	33
Fe–Cr alloys	Fe–Cr alloys	Weight loss	Phase interaction	34
Ag, Au, Al, Ti, Pt, Fe, Cu, Zn	Minerals	E_{corr}, *E–I* curves	Processing equipment	35
		Salt Solutions		
Al, Cd films	4340 steel	I_g, E_g, stress	Hydrogen embritt.	36
SiC	Mg alloys	I_g, i_{corr}	Composite material	37
Steel	Al, Zn	Weight loss, *E–I* curves	Mechanism	38
Steel	Al	E_g, I_g, weight loss	pH, dissov. oxygen	39
Steel	G. steel	I_g	Corrosion products	40
Steel	G. steel	E_a, E_c, I_g, *E–I* curves	Zn coating composition	41
Steel	Zn coating	I_g	Effect of paint	42
Steel	G. steel	I_g	Polarity reversal	43

TABLE 10.1. (*Continued*)

Alloy 1	Alloy 2	Measurements[a]	Focus	References
Steel	Zn alloys	Weight loss	Solution composition	44
Steel	Cd, Zn, Al	Cracking	SCC protection	45
Al, Ti alloys, Pt, Cu	Cu, Zn, Fe	I_g	Current measurement	46
S. steel	Graphite-epoxy	E_g, I_g, E_{corr}	Area effect	47
Al alloys, S. steels	Graphite-epoxy	I_g	Composite materials	48, 49
Al alloys	Cu, Cd, Zn, Ti, steels	I_g	Area effect	50
Al alloys	Ag, Cu, Ni, Sn, Zn	E_g, I_g	Galvanic series	51
Al	Graphite, TiB, SiC	E_{corr}, E_g, I_g	Composite materials	52, 53
Cu	Zn	E, I distributions	Solution resistance	54
Cu	Zn	E distribution	Modeling	55
Cu, Brass	Zn	E distribution, I_g	Corrosion rate	56
Al, Ti, Fe, Ni, Cu, S. steel	Oxides	I_g, E–I curves	Corrosion products	57
Cu	Zn	E distribution	Geometry analysis	25
Sn, Cd, Zn, Steel	S. Steel, Ni, Cu, Ti, Sn, steel, Zn	E_g, I_g, weight loss	Corrosion rate	58
G. steel, S. steel	Polyethylene	I_g	Telephone cable	59
Al, Au, Ag, Pt, Si, Mg, Cu		E_{corr}	Galvanic series	60
		Other Environments		
S. steel[b]	Ti, Nb, Ta	E_g, I_g	Biocompatibility	61
Cu[c]	Zn	E distribution	Kelvin probe	62
Steel[d]	Zn	E_c, I_g	Cathodic protection	63
Steel[e]	Zn	Morphology	Paint adhesion	64
Steel[f]	Zn	Morphology	Humidity, time	65
S, steel[g]	S. steel	E_{corr}, I_g, E–I curves	Abrasion–corrosion	66
Miscellaneous	Miscellaneous	E_{corr}, E–I curves	Review	21
Steel, S. steels[h]	Steel, S. steels	Weight loss	Database	67
Steel[d]	Zinc	Weight loss	Galvanic protection	68
Zinc	Miscellaneous	Miscellaneous	Review	69

[a] I_g galvanic current; E_g, potential of couple; E_c, potential of cathode; E_{corr}, corrosion potential; E_a potential of anode; S. steel, stainless steel; G. steel, galvanized steel; i_{corr} corrosion current.
[b] Ringer's solution.
[c] Humid gas.
[d] Concrete.
[e] Painted.
[f] Cyclic test.
[g] Wet minerals.
[h] Oil and gas.

C. FACTORS IN GALVANIC CORROSION

Many factors play a role in galvanic corrosion in addition to the potential difference between the two coupled metals. Depending on the circumstances, some or all of the factors illustrated in Figure 10.1 may be involved. Generally, for a given couple, the factors in categories (a)–(c) vary less from one situation to another than the factors in categories (d)–(g). Effects of geometric factors on galvanic actions can, in many cases, be mathematically analyzed. On the other hand, effects of electrode surface conditions on reaction kinetics in real situations can be very difficult to determine. Compared to normal corrosion, galvanic corrosion is generally more complex because, in addition to material and environmental factors, it involves geometrical factors.

D. MATERIAL FACTORS

D1. Effects of Coupled Materials

As listed in Figure 10.1, all the factors affecting the electrode properties, such as those under categories (a)–(g), have an influence on galvanic action between any two metals. The reversible electrode potentials of the two coupled metals determine the intrinsic polarity of a galvanic couple, whereas the reactions, metallurgical factors, and surface conditions determine the actual polarity under a given situation because the actual potential (the corrosion potential) of a metal in an electrolyte is usually very different from its thermodynamic equilibrium value due to kinetic processes. For example, titanium has a very negative reversible electrode potential

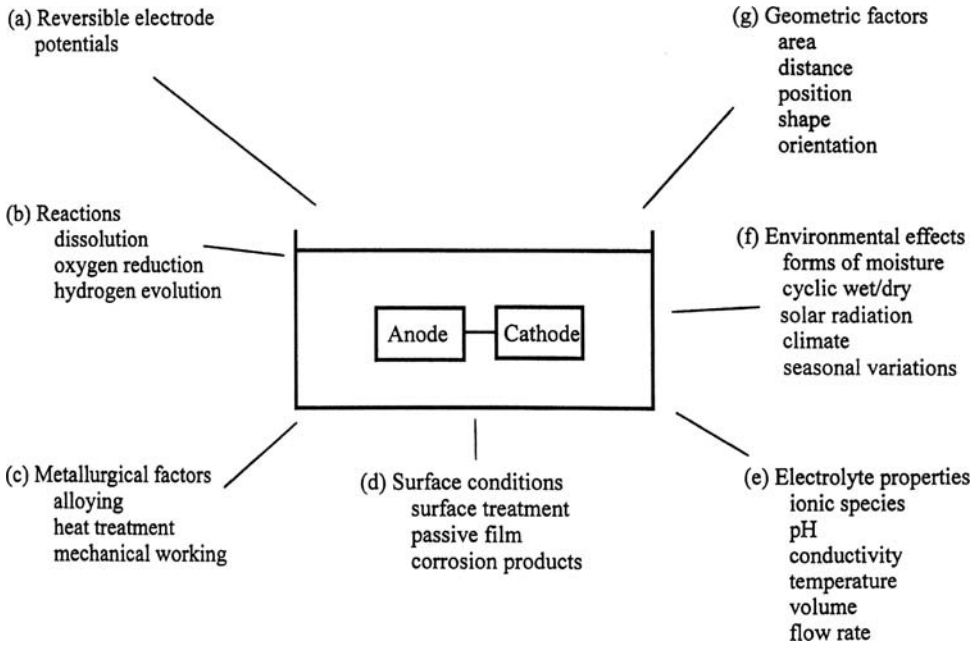

FIGURE 10.1. Factors involved in galvanic corrosion of bimetallic couple.

and has an active position in the emf series. However, titanium occupies a noble position in the galvanic series in many practical environments due to passivation of the surface.

The extent of galvanic activity is not always related to the difference in the corrosion potentials of two metals. Table 10.2 shows that, for steel, the galvanic corrosion is much higher when coupled to nickel and copper than when coupled to 304 stainless steel and Ti–6Al–4V, for which the potential differences were larger. The galvanic corrosion of zinc is the highest when coupled to steel, although the potential difference between zinc and steel is much less than between zinc and most other alloys.

Similar results have been reported on galvanic corrosion in atmospheres [2] where, in addition to the potential differences between the two metals, other factors, such as reaction kinetics and formation of corrosion products, are important in determining the galvanic corrosion rate. When the cathodic reaction is oxygen reduction and diffusion limited, different galvanic corrosion rates of an anode, coupled to different cathode materials, can be explained by the different diffusion rates of oxygen through the oxide films. When diffusion is not the limiting process, differences in galvanic corrosion rates can result from differences in cathodic efficiency of oxygen reduction in the oxide scale on the cathode surface [58], which may not depend on the corrosion potential. The difference in corrosion potentials of uncoupled metals is, thus, not a reliable indicator of the rate of galvanic corrosion.

The extent of galvanic corrosion can be ranked with actual corrosion loss data (i.e., the increase in corrosion rate relative to uncoupled conditions) [51, 58]. There is a difference between the corrosion loss determined by weight loss, which includes the loss due to local corrosion, and due to galvanic current, which measures the true loss due to galvanic action. As noted in Table 10.2, the weight loss of zinc, when galvanically coupled to other metal alloys, can be much larger than the sum of the galvanic corrosion calculated from

TABLE 10.2. Galvanic Corrosion Rate of Steel and Zinc Coupled to Various Metal Alloys Tested in 3.5% NaCl Solution[a,b]

Coupled Alloy	r_g[c] (μm/year)	r_{wl}[d] (μm/year)	ΔV[e] (mV)
	4130 Steel, $r_0 = 90$		
SS 304	119	625	−439
Ti–6A1–4V	79	589	−338
Cu	343	1260	−316
Ni	341	1050	−299
Sn	122	581	−69
Cd		38	+221
Zn		14	+483
	Zn, $r_0 = 101$		
SS 304	244	705	−905
Ni	990	1390	−817
Cu	1065	1450	−811
Ti–6A1–4V	315	815	−729
Sn	320	810	−435
4130 steel	1060	1550	−483
Cd	600	660	−258

[a]Tested for 24 h, equal size surface area of 20 cm^2.
[b]See [58].
[c]Measured as galvanic current.
[d]Measured as weight loss.
[e]Potential difference between the coupled metals before testing.

the Faradaic current plus the normal corrosion measured in an uncoupled condition. This indicates that the local corrosion of zinc is increased by galvanic coupling to another alloy. Some of the factors that determine the relationship of galvanic current and weight loss have been discussed in the literature [51].

In general, addition of small amounts of alloying elements does not change the reversible potential of a metal to a large extent, but may change significantly the kinetics of the electrochemical processes and, thus, behavior in galvanic action. For example, significant differences have been found in the corrosion behavior of different aluminum alloys in galvanic couples [51].

For alloys with a microstructure of more than two phases, there can be significant galvanic action among the different phases. Microscale galvanic action has been studied for the active dissolution of duplex stainless steel in acidic solutions [34] and for the interaction between martensite and ferrite in grinding media [66]. Potential and current distributions on the surface of a metal, consisting of two randomly distributed phases, have been mathematically modeled by Morris and Smyrl [70].

Increased corrosion of the cathodic member in a galvanic couple may also occur (e.g., the zinc–aluminum couple). Although aluminum is cathodic to zinc in 3.5% solution, the rate of aluminum corrosion is greater when coupled to zinc than in the uncoupled condition [51]. The higher corrosion rate of the coupled aluminum is attributed to die increased alkalinity near the surface due to the cathodic reaction, since aluminum is not stable in a solution of high alkalinity. Similar effects have been reported for tin–zinc and cadmium–zinc couples, where the corrosion of tin and cadmium, being the cathodic members, in 3.5% NaCl solution increased compared to the uncoupled condition [58].

Historically, galvanic corrosion has been reported to occur mostly in bimetallic couples. With the ever-increasing use of nonmetallic materials, galvanic corrosion is now being identified in many situations where a metal is in contact with a nonmetallic material (e.g., galvanic corrosion of metals occurs in metal-reinforced polymer matrix composites and graphite metal matrix composites [49, 53], in processing of semiconducting minerals [35], in contact with conducting polymers [59], with semiconducting metal oxides [57], and with conducting inorganic compounds [8]). It has been found that minerals, in general, exhibit potentials more noble than most metals and, therefore, may cause galvanic corrosion of metals used in processing equipment [35].

D2. Effect of Area

The effect of anode and cathode areas on galvanic corrosion depends on the type of control in the system, as illustrated later in Figure 10.10. If the galvanic system is under cathodic control, variation in the anode area has little effect on the total rate of corrosion, but variation of the cathode area has a significant effect. The opposite is true if the system is under anodic control.

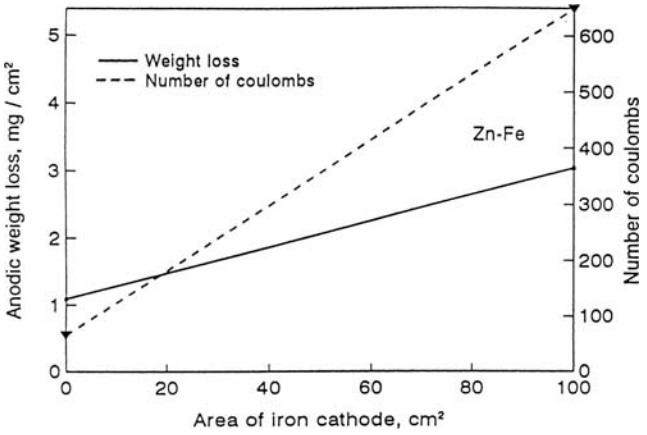

FIGURE 10.2. Effect of area of mild steel cathode on weight loss of Zn anode (area of 100 cm^2) and on number of coulombs flowing between Zn–steel couple over a 96-h period in 1 *N* NaCl solution at 25°C [38].

Galvanic currents in many situations are proportional to the surface area of the cathode (e.g., Figure 10.2 shows that the galvanic corrosion of zinc increases with increasing iron cathode area). On the other hand, the galvanic corrosion of zinc changes only very slightly with increasing zinc anode area. These results indicate that the galvanic corrosion of zinc in the system is mainly cathodically controlled. Similar results were found for aluminum alloys, coupled to copper, stainless steels, or Ti–6A1–4V, where the total galvanic current is independent of the surface area of the anode but is proportional to the cathode area [50].

D3. Effect of Surface Condition

The surface of metals in contact with an electrolyte is generally not "bare" but is covered with a surface layer, at least an adsorption layer, but often a solid surface film. This is the most important factor that causes the difference between the intrinsic polarity and apparent polarity and between the difference in potentials and the extent of galvanic corrosion. Formation of a surface film, whether a salt film or an oxide film, may significantly change the electrochemical properties of the metal surfaces, resulting in very different galvanic action.

A corrosion product film may serve as a physical barrier between the metal surface and the environment. It may also be directly involved in the electrochemical reactions if it conducts electrical current, either as a conductor or a semiconductor. Most metal oxides, common corrosion products, are conductive materials, mainly as semiconductors [71]. Depending on the electronic structure, oxide films exhibit potentials that are generally very different from the base metals. In many situations, these oxides, rather than the

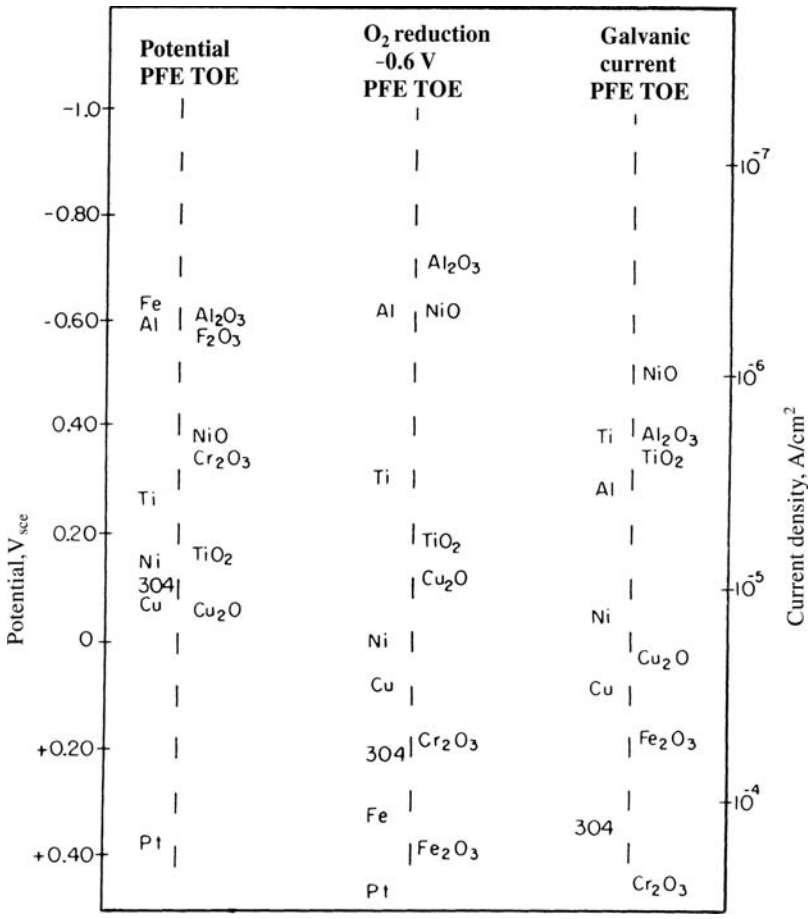

FIGURE 10.3. Corrosion potentials and oxygen reduction rates of metal oxides. PFE: passive film electrode; TOE: thermal oxide electrode [57], (Copyright ASTM. Reprinted with permission.)

metals themselves, determine the electrode potential and the position in a galvanic series. Figure 10.3 shows a galvanic series and the cathodic efficiency for O_2 reduction on a number of metal oxides [57]. The highest current densities for O_2 reduction are observed for *n*-type semiconductor oxides (Fe_2O_3) and metal-like oxides (Cr_2O_3). Insulators (Al_2O_3) and *p*-type oxides (NiO) are inefficient cathodes. The oxides, having a high cathodic efficiency and exhibiting a more noble potential value in a galvanic couple, result in a larger galvanic corrosion rate of the coupled metal.

According to Stratman and Müller [72], oxygen reduction of an iron electrode is greatly increased due to the formation of rust because oxygen can be reduced in the iron oxide scale, which is generally porous and has a large effective surface area. The corroded steel surface is, thus, a highly effective cathode when coupled to metals that have more negative potentials, such as zinc, aluminum, and magnesium [40, 73].

Surface passivation is important in the galvanic action of a bimetallic couple (e.g., aluminum is normally passivated in neutral aqueous solutions), but the extent of passivity is relatively low in solutions containing species such as chloride ions and may break down under certain conditions. When aluminum is coupled to steel, it acts as an anode in chloride solutions, whereas it acts as a cathode in tap water and distilled water [37].

When a surface film does not fully cover the entire surface, part of the metal surface is passivated and acts as the cathode, forming a local galvanic cell, increasing the corrosion rate of the nonpassivated part of the surface, and possibly causing pitting corrosion [57]. For example, galvanic current develops between a passivated zinc sample and a partially passivated zinc sample in a cell of two compartments, containing $0.1\,M$ K_2CrO_4 in one and $0.1\,M$ K_2CrO_4 and NaCl in the other, respectively [74], Pitting occurred on the sample placed in the compartment containing NaCl [74].

When considering surface condition, the effects of time should also be included. With the passage of time, two basic changes invariably occur in a corrosion system: (1) a change of the physical structure and chemical composition of the corroding metal surface and (2) a change in the composition of the solution, particularly in the vicinity of the surface [75]. Specific changes may occur in surface roughness and area,

adsorption of species, formation of passive films, saturation of dissolution products, precipitation of a solid layer, and exhaustion of reactants. Mechanistically, these changes may lead to alterations in the equilibrium potentials, the type of reactions involved, the rate-controlling process, and so on. As a result, the corrosion potential may vary greatly depending on the nature and extent of these changes.

The steady-state corrosion potential of a metal electrode depends on whether the surface is active or passive, and the time required for reaching a steady-state value varies with the conditions. The rate of galvanic corrosion may change with time as a result of changes in polarity and in potential difference between the metals in the couple. It has been reported that the potentials of various bimetallic couples, including iron, stainless steel, copper, bronze, and zinc, exposed in flowing seawater are highly variable, and the galvanic currents are reduced by about one order of magnitude within the first 120 days [26].

E. ENVIRONMENTAL FACTORS

A corrosive environment is characterized by its physical and chemical nature, which may affect the electrochemical properties. Given that the electrochemical properties of each metal are distinctive in a given electrolyte, galvanic corrosion is essentially unique for each metal couple in each environment. The combination of metal couples and environmental conditions is, thus, limitless, as can be appreciated from Table 10.1.

E1. Effects of Solution

As discussed in Section D, galvanic action of a bimetallic couple depends on the surface condition of the metals, which, in turn, is determined by environmental conditions. A metal surface exhibits different potentials in different electrolytes, as shown in Table 10.3, which lists the corrosion potentials of a number of metals in four different electrolytes of similar ionic strength. A galvanic series provides information on the polarity of a bimetallic couple but is environment-specific because the relative position of each metal changes with solution.

The extent of galvanic corrosion also varies with solution composition. The corrosion rates of zinc and steel in coupled and uncoupled conditions in several solutions [44] can be seen in Table 10.4. In all the solutions, galvanic action results in protection of the steel, but the amount of zinc corrosion

TABLE 10.3. Corrosion Potentials (mV_{sce}) of Metals after 24-h Immersion in Four Different Solutions, Compared with the emf Series[a]

emf	0.1 *M* HCl	0.1 *M* NaCl	0.1 *M* Na_2SO_4	0.1 *M* NaOH
Ag +799	Ag +48	Ag –60	Ag +147	Ag –64
Cu +324	Ni –135	Ni –142	Cu –43	S. steel –96
Pb –126	Cu –139	Zr –150	Cr –45	Ni –171
Sn –138	Ta –213	Cu –189	Ti –66	Cu –231
Ni –257	Ti –221	Cr –270	Ni –70	Cr –303
In –338	Zr –297	Ti –272	Ta –154	Fe –389
Fe –447	Cr –347	Ta –295	Zr –218	Ta –500
	S. steel –473	S. steel –320	S. steel –348	Zn –555
Cr –744	Pb –487	Pb –565	Sn –421	Ti –591
Ta –750	Sn –497	Sn –565	Al –505	In –600
Zn –762	Fe –557	In –646	Pb –545	Zr –631
Zr –1553	In –680	Fe –710	In –651	Pb –757
Ti –1630	Al –731	Al –712	Fe –720	Mg –809
Al –1660	Zn –989	Zn –1019	Zn –1049	Sn –1096
Mg –2370	Mg –1894	Mg –1548	Mg –1588	Al –1351

[a]Sample surface area about 1 cm^2; polished with 600-grade emery paper; solution open at air at room temperature.

TABLE 10.4. Corrosion Rate of a Zinc–Steel Couple in Various Solutions (μm/year)[a, b]

	Uncoupled		Coupled	
Solution	Zinc	Steel	Zinc	Steel
0.05 *M* $MgSO_4$	+	66	86.4	+
0.05 *M* Na_2SO_4	285	254	838	+
0.05 *M* NaCl	254	254	762	+
0.005 *M* NaCl	112	178	218	+
Carbonic acid	10.2	73.7	38.1	+
Calcium carbonate	+	150	+	+
Tap water	+	71.1	+	+

[a]See [44].
[b]Specimen of equal surface area partially immersed for 39 days. Plus signs indicate specimens gained weight.

varies with solution composition. The difference in the corrosion rates in magnesium sulfate and sodium sulfate solutions indicates the significant effect of cations on the reaction kinetics.

The conductivity of the electrolyte is a very important factor because it determines the distribution of galvanic corrosion across the anode surface. When conductivity is high, as in seawater, the galvanic corrosion of the anodic metal is distributed uniformly across the surface. As the conductivity decreases, galvanic corrosion becomes concentrated in a narrow region near the junction, as illustrated in Figure 10.4. Usually, the total galvanic corrosion is less in a poorly conducting electrolyte than in a highly conducting one.

Ions of noble elements in solution may cause galvanic corrosion of a less noble metal immersed in the solution because precipitation of the noble element can cause small galvanic cells to form [76].

If there is only a limited amount of electrolyte, the composition of the electrolyte may significantly change as a result of electrochemical reactions. Massinon et al. [77, 78] found an increase of pH in a confined electrolyte after a certain time of galvanic action for a zinc–steel couple. Pryor and Keir [79] pointed out that, when the distance between the anode and cathode is small compared to the dimension of the electrodes, the galvanic corrosion is small due to the limitation in the mass transport of the reactants and reaction products.

One important solution factor is the thickness of thin-layer electrolytes, which is encountered in atmospheric environments. The thickness of an electrolyte affects corrosion processes in several different ways. First, it affects the lateral resistance of the electrolyte and, thus, affects the potential and current distribution across the surface of the coupled metals. Second, it affects the transport rate of oxygen across the electrolyte layer and, thus, the rate of cathodic reaction. Third, it changes the volume and the solvation capacity of the electrolyte and, thus, affects the formation of corrosion products.

As shown later in Figures 10.11 and 10.12, changes in potential and galvanic current across a metal surface are greater for thinner electrolytes due to the larger electrical resistance involved. Under a thin-layer electrolyte, the galvanic corrosion is the most intense at the anode area near the anode–cathode boundary, while there is very little galvanic corrosion away from the boundary, as illustrated in Figure 10.4(a). Variation of electrolyte thickness also determines the rate-controlling process for a given cell dimension. Figure 10.5 shows that, for a thinner electrolyte, the galvanic current is larger when the anode and the cathode are close, but the reverse applies when the two electrodes are far apart [80]. Since the oxygen diffusion rate under thin-layer electrolytes changes with electrolyte thickness, the change of the relative galvanic current values for small and large distances, shown in Figure 10.5, is due to the change of the rate-limiting process from oxygen diffusion at a close distance to ohmic conduction in the electrolyte at a large distance [80].

The physical position of a galvanic couple in solution can also affect the galvanic action between coupled metals. Shams El Din et al. [74] found a large potential variation near the solution surface between a zinc anode and a copper cathode that were half-immersed in solution, due to the higher oxygen concentration near the surface than in the bulk solution.

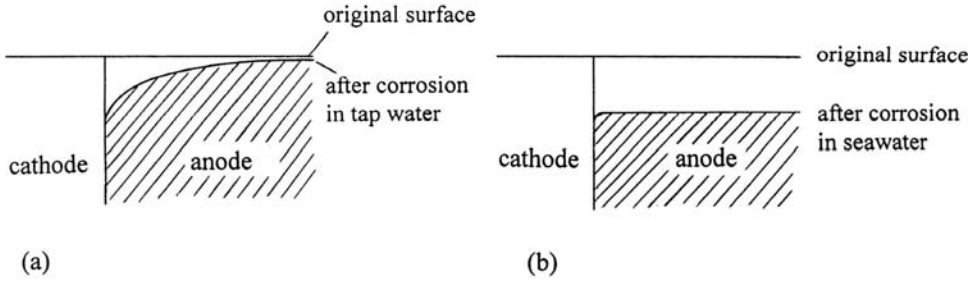

FIGURE 10.4. Effect of solution conductivity on distribution of galvanic corrosion: (a) low conductivity and (b) high conductivity.

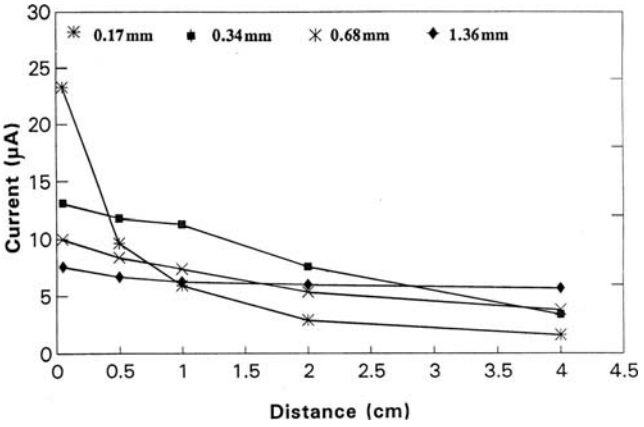

FIGURE 10.5. Galvanic current as function of distance between zinc and steel in 0.001 M Na_2SO_4 solutions of different electrolyte thickness [80]. [Reprinted from *Corrosion Science*, **34**, X. G. Zhang and E. M. Valeriote, "Galvanic Protection of Steel and Galvanic Corrosion of Zinc under Thin Layer Electrolytes," p. 1957 (1993), with permission from Elsevier Science.]

E2. Atmospheric Environments

Galvanic corrosion occurs commonly in atmospheric environments as different combinations of materials are used in buildings and structures exposed to indoor and outdoor atmospheres. A test program of galvanic corrosion in atmospheres was started as early as 1931 by the American Society for Testing and Materials (ASTM) [2]. Since then, a number of extensive exposure programs have been carried out all over the world [81–84]. The various aspects of atmospheric galvanic corrosion have been discussed in a comprehensive review by Kucera and Mattsson [2].

Galvanic corrosion under atmospheric environments is most often evaluated by weight loss measurement. In other environments, potentials and/or galvanic currents of coupled metals can be measured, but it is very difficult to measure in situ potentials of metals under atmospheric conditions due to the thin layer of the electrolyte.

Data in Table 10.5, reported by Kucera and Mattsson [2], show the galvanic corrosion rates of a number of metal alloys, in the form of wire coupled to bolts of various metals. Depending on the bolt metal and the type of atmosphere, the galvanic corrosion rate of the wire can be many times that of the normal corrosion rate. For example, the galvanic corrosion of zinc is as much as five times the normal corrosion in a rural atmosphere and three times that in a marine atmosphere [85]. The amount of corrosion shown in Table 10.5 does not appear to relate to differences between the reversible potentials of the coupled metals. Steel and copper, as cathodic members of a couple, cause the most galvanic corrosion of the coupled anodic material.

Galvanic corrosion in atmospheres is usually restricted to a narrow region of the anode metal near the bimetallic junction because of the high resistance of thin-layer electrolytes formed by rain and water condensation [80, 86, 87]. Even for the most incompatible metals, direct galvanic action will not extend more than a few millimeters from the junction. Because of the very narrow range of galvanic action, geometrical factors of the coupled metals, such as shape and size, generally do not have a strong effect on galvanic corrosion in atmospheric environments.

Galvanic action is most significant in marine atmospheres because of the high conductivity of seawater. Compared to other types of moisture formed under atmospheric conditions, rain is particularly effective in causing galvanic corrosion. The galvanic corrosion rate is several times that of the normal corrosion rate in an open exposure, whereas they are similar when under a rain shelter because the electrolyte layer formed by rain is thicker and has a smaller lateral electric resistance than the moisture formed by condensation [2].

E3. Natural Waters

Natural waters are commonly classified as seawater and freshwater, such as river, lake, and underground waters. A distinct difference between seawater and freshwater is that seawater has a high conductivity due to its high salt content, whereas freshwaters generally have low conductivities. In comparison to other environments, waters as corrosion

TABLE 10.5. Corrosion Rate (μm/year) of Wire Specimens Coupled to Bolts of Other Materials Exposed for 1 Year in an Urban Environment[a]

Bolt	Nylon	Steel	S. Steel	Cu	Pb	Zn	Ni	Al	Sn	Cr	Mg
Wire											
Steel	25.7		31	32	23	1.2	29	22	32	27	0.6
S. steel				0.2			0.2			0.02	
Cu		0.3	1.0		0.6		1.0		0.7	0.4	0.1
Zn	1.2	3.3	1.8	2.0	2.4		1,9	1.1	2.6	1.4	0.04
Ni			1.3	0.1						1.0	
Al	0.2	1.8	0.6	5.3	0.6	0.0	0.6		0.6	0.3	0.0
Sn		0.4	1.5	3.5		0.0	1.5	0.4		0.3	0.0
Mg		18	10	10	13	9.0	20	5.3	8.1	9.2	

[a]See [2].

TABLE 10.6. Galvanic Series of Some Commercial Metals and Alloys in Seawater[a]

	Platinum
↑	Gold
Noble or	Graphite
cathodic	Titanium
	Silver
	Chlorimet 3 (62 Ni–18 Cr–18 Mo)
	Hastelloy C (62 Ni–17 Ct–15 Mo)
	18-8 Mo stainless steel (passive)
	18-8 stainless steel (passive)
	Chromium stainless steel 11–30% Cr (passive)
	Inconel (passive) (80 Ni–13 Cr–7 Fe)
	Nickel (passive)
	Silver solder
	Monel (70 Ni–30 Cu)
	Cupronickels (60–90 Cu–40–10 Ni)
	Bronzes (Cu–Sn)
	Copper
	Brasses (Cu–Zn)
	Chlorimet 2 (66 Ni–32 Mo–1 Fe)
	Hastelloy B (60 Ni–30 Mo–6 Fe–1 Mn)
	Inconel (active)
	Nickel (active)
	Tin
	Lead
	Lead–tin solders
	18-8 Mo stainless steel (active)
	18-8 stainless steel (active)
	Ni-Resist (high Ni cast iron)
	Chromium stainless steel, 13% Cr (active)
	Cast iron
	Steel or iron
	2024 aluminum (4.5 Cu, 1.5 Mg, 0.6 Mn)
Active or	Cadmium
anodic	Commercially pure aluminum (1100)
↓	Zinc
	Magnesium and magnesium alloys

[a]See [88]. Reprinted from M. G. Fontana and N. D. Greene, *Corrosion Engineering*, 2nd ed., 1978, McGraw–Hill, with permission of The McGraw–Hill Companies.

environments are homogeneous (e.g., seawater is almost constant with respect to time and geographic location). The galvanic action in seawater, due to its high conductivity and uniformity, is long range and spreads uniformly across the entire surface area of a metallic structure. The galvanic effect in freshwaters is generally much less than in seawater because of the lower conductivity [14].

Table 10.6 presents the galvanic series of some commercial metals and alloys obtained in seawater [88]. As discussed previously, such a galvanic series differs from the emf series and is specific to seawater. A galvanic series of a number of common alloy couples in flowing seawater has also been reported [26, 89, 90].

Galvanic corrosion in seawater has been extensively investigated, as indicated in Table 10.1. Table 10.7 shows the data on the galvanic action of various bimetallic couples after long-term exposure in seawater and freshwater [14]. Galvanic action is much stronger in seawater than in freshwater. In seawater, the corrosion rate of an anodic metal, such as zinc or steel, is larger by a factor of 5–12 than in the uncoupled condition, whereas the increase is a factor of only 2–5 in freshwater. The data also indicate the great effect of the relative sizes of the anode and cathode; a factor of 6–7 times more corrosion was observed on the anode by changing the anode from the strip to the plate for the same bimetallic couple (e.g., 316 stainless steel/carbon steel, phosphor bronze/carbon steel, and 316 stainless steel/phosphor bronze). Table 10.7 also indicates that the corrosion of the cathodic member was generally decreased, in varying degrees, as a result of the galvanic corrosion of the anodic member.

F. POLARITY REVERSAL

The normal polarity of some galvanic couples under certain conditions may reverse with the passage of time. This phenomenon was first reported by Schikorr in 1939 on a zinc–steel couple in hot supply water with iron becoming anodic to zinc, which has been a serious problem for galvanized steel hot water tanks [91]. It has subsequently been extensively investigated [10, 12, 43].

Polarity reversal is invariably caused by the change of surface condition of at least one of the coupled metals, such as formation of a passive film. The degree of passivity, the nature of the redox couples in the solution, and the stability of the system determine the polarity and its variation with time. For a zinc–steel couple, the change in the zinc electrode potential is chiefly responsible for the reversal of polarity since the potential of the steel remains relatively unchanged with time in hot water [12]. It has generally been found that polarity reversal does not occur in distilled water up to 65°C and without the presence of oxygen [12, 43, 92].

Depending on the conditions, it may occur rather quickly, taking several minutes, or rather slowly, taking many days. In addition to temperature, other factors, such as dissolved ions, pH, and time of immersion, affect the polarity of a zinc–steel couple. The necessary conditions for polarity reversal of a zinc–steel couple are passivation of the zinc surface and sufficient reducing species, such as dissolved oxygen, in the water to provide cathodic depolarization.

Polarity reversal of an aluminum–steel couple has also been found to occur in natural environments where aluminum alloys are used as anodes for cathodic protection of steel. The general mechanism is similar to that occurring with a zinc–steel couple. However, unlike zinc, aluminum is normally passivated by a thin oxide film in most natural environments. The potential of aluminum depends on the degree of passivity, which is sensitive to the ionic species

TABLE 10.7. Galvanic Corrosion of Various Metal Alloys in Seawater and Freshwaters After 16 Years Exposure[a,b]

Strip/Plate[c]	Seawater	Freshwater
316 S. steel/carbon steel	0.1/49.5(2.0, 48.1)	0.0/32.4 (0.0, 26.0)
316 S. steel/naval brass	0.0/16.2 (2.0, 12,4)	0.0/2.5 (0.0,1.9)
316 S. steel/phosphor bronze	0.0/9.4 (2.0, 5.5)	0.0/0.7 (0.0, 0.7)
Phosphor bronze/carbon steel	0.4/55.1 (5.5, 48.1)	0.1/28.9 (0.7, 26.0)
Phosphor bronze/aluminum	0.7/6.5 (5.5, 1.0)	0.1/12.4 (0.7, 5.0)
Phosphor bronze/2% Ni steel	0.5/60.8 (5.5, 52)	0.2/24.6 (0.7, 21.1)
Phosphor bronze/cast steel	0.2/51.6 (5.5, 43.3)	0.1/30.1 (0.7, 26.3)
Phosphor bronze/302 S. steel	21.9/6.3 (5.5, 9.3)	3.8/0.0 (0.7, 0.0)
Phosphor bronze/316 S. steel	41.3/0.2 (5.5, 2.0)	1.8/0.0 (0.7, 0.0)
Phosphor bronze/70 Cu–30 Ni	4.6/3.8 (5.5, 2.3)	0.5/1.3 (0.7, 1.3)
Phosphor bronze/monel	71.8/7.0 (5.5, 8.7)	14.1/0.8 (0.7, 0.6)
Carbon steel/aluminum	1.6/7.8 (48.1, 0.9)	17/9.4 (26.0, 1.5)
Carbon steel/2%Ni steel	63.1/48.2 (48.1, 52)	33.9/19.1 (26.0, 22.9)
Carbon steel/70 Cu–30 Ni	310[d]/1.6 (48.1, 2.3)	68.2/0.3 (26.0, 1.3)
Carbon steel/nickel	320[d]/4.8 (48.1, 19)	71.3/0.2 (26.0, 0.0)
Carbon steel/copper	350[d]/2.9 (48.1, 6)	77.7/0.2 (26.0, 1.0)
Carbon steel/phosphor bronze	318[d]/1.9 (48.1, 5.5)	65.5/0.3 (26.0, 0.7)
Carbon steel/302 S. steel	298[d]/0.8 (48.1, 9.5)	52.7/0.0 (26.0, 0.0)
Carbon steel/316 S. steel	260[d]/0.0 (48.1, 2.0)	44.4/0.0 (26.0, 0.0)
Carbon steel/20%Zn brass	281[d]/2.4 (48.1, 3.7)	63.4/0.3 (26.0, 1.7)
Zinc/carbon steel	5/15.5 (14.9, 48.1)	43.1/19.9 (7.9. 26.0)
Zinc/2%Ni steel	l87[d]/14.9 (14.9, 52)	36.6/17.4 (7.9, 22.8)
Zinc/cast steel	198/11.4 (14.9, 43.3)	45.6/21.9 (7.9, 26.3)
Zinc/18% Ni cast iron	167[d]/0.1 (14.9, 22.8)	23.7/7.7 (7.9, 8.0)

[a]See [97].
[b]Average penetration m mils (1 mil = 25.4 μm), the values in parentheses are the corrosion loss of the allays in uncoupled conditions.
[c]Strip area = 141 cm^2, plate area = 972 cm^2, carbon steel (0.24%C), 316 S. steel (18Cr–1.3Mo), 302 S. steel (18 Cr–8 Ni), phosphor bronze (4 Sn–0.25 P), low brass (20%Zn), aluminum (99%), zinc (99.5%), lead (99.5%), aluminum bronze (5%Al), Monel (70 Ni–30 Cu).
[d]Estimated according to the data at 8 years.

in the environment. For example, carbonate and bicarbonate ions promote passivity and, thus, produce more noble potential values, whereas ions like chloride give the opposite effect [15]. In practice, sacrificial aluminum anodes are alloyed with various elements to prevent reversal of polarity.

The consequence of polarity reversal can be serious. In the zinc–steel and the aluminum–steel couples, zinc and aluminum serve as sacrificial anodes for protecting the steel. Polarity reversal results in the loss of cathodic protection of steel, causes galvanic corrosion of the steel, and shortens the life of the steel structure.

G. PREVENTIVE MEASURES

The essential condition for galvanic corrosion to occur is two dissimilar metals that are both electrically and electrolytically connected. Theoretically, prevention of galvanic corrosion can be achieved by avoiding the use of dissimilar metals in an assembly, by electrically separating the dissimilar metals with an insulating material or by physically insulating the environment from the metal surface with a coating impermeable to water. In reality, however, complete prevention is often not practical, as dissimilar metals need often to be used in direct contact and exposed to a corrosive environment and there is no absolutely impermeable coating. Thus, measures to minimize the possibility and extent of galvanic corrosion must be implemented All the factors listed in Figure 10.1 can be considered and controlled in order to reduce galvanic corrosion. Some practical approaches are as follows:

(a) Avoid combinations of dissimilar metals that are far apart in the galvanic series applicable to the environment.
(b) Avoid situations with small anodes and large cathodes.
(c) Isolate the coupled metals from the environment.
(d) Reduce the aggressiveness of the environment by adding inhibitors.
(e) Use cathodic protection of the bimetallic couple with a rectifier or a sacrificial anode.
(f) Increase the length of solution path between the two metals. This method is beneficial only in electrolytes

of low conductivity, such as freshwaters, because strong galvanic action exists several meters away in highly conductive media, such as seawater.

The use of these approaches must meet the specific requirements of each application [93, 94]. Sometimes one is sufficient, but a combination of two or more may be required in other situations. It must be emphasized that the most effective and efficient way to prevent or minimize galvanic corrosion is to consider the problem and take measures early in the design stage.

H. BENEFICIAL EFFECTS OF GALVANIC CORROSION

As a result of galvanic corrosion of the anodic metal, the corrosion of the cathodic, coupled metal or alloy is generally reduced (i.e., cathodically protected). This effect has been well utilized in the application of sacrificial anodes, coatings, and paints for corrosion protection of many metal components and structures in various environments.

Sacrificial anodes, mainly made of zinc, aluminum, and magnesium and their alloys, are widely used in corrosion prevention underwater and underground for structures such as pipelines, tanks, bridges, and ships. Each alloy possesses a unique set of electrochemical and engineering properties and has its own characteristic advantages as an anode for galvanic protection of a more noble alloy, mostly steel, in a given situation [95, 96]. Anodes can be designed for composition, shape, and size according to specific applications [95].

Galvanized (i.e., zinc coated) steel is a typical example of a metallic coating that provides a barrier layer to protect the steel and also sacrificially protects the locations where discontinuities occur in the coating [39, 97]. The combination of barrier and galvanic protection by the zinc coating results in very effective corrosion protection of steels. Table 10.8 shows that galvanic corrosion resulted in a reduction of the corrosion of steel by 3 times in rural, 40 times in industrial, and 300 times in seacoast industrial atmospheres. On the other hand, the galvanic corrosion of zinc, an increase of corrosion by a factor of 1.6–3 compared to uncoupled conditions, is very little compared to the reduction of steel corrosion. Galvanic protection of the steel is more effective in industrial and marine atmospheres than in rural ones, suggesting that the pollutants in the atmospheres are beneficial to the galvanic protection of steel, although they are very harmful to the normal corrosion of the uncoupled steel.

The protection distance of steel by a zinc coating in atmospheric environments is limited to a region only a few millimeters from the zinc coating because of the high resistance of thin-layer electrolytes formed in the atmosphere [87]. The protection distance, as a function of electrolyte thickness and surface area of steel, is shown in Figure 10.6. Figure 10.7 shows the protection distance as a function of separation distance and width of steel determined in an atmospheric environment [86]. The data indicate that the largest protection distance is $\sim$1 mm, implying that the width of a scratch on a zinc-coated steel, which is fully protected is $\sim$2 mm in the atmosphere. However, the actual protected area, which also includes the areas under partial protection, is considerably larger [86].

I. FUNDAMENTAL CONSIDERATIONS

I1. Electrode Potential and Kirchhoff's Law

The direction of galvanic current flow between two connected bare metals is determined by the actual electrode potentials (i.e., corrosion potentials of the metals in a corrosion environment). The metal which has a higher (i.e., more positive, more noble, or more cathodic) electrode potential is the cathode in the galvanic couple, and the other is the anode.

The polarity of galvanic couples in real situations may be different from that predicted by the thermodynamic reversible potential in the emf series, because the corrosion potentials are determined by the reaction kinetics at the metal– electrolyte interface. Thus, the actual position of each metal or alloy in a specific environment forms a galvanic

TABLE 10.8. Corrosion of Galvanic Couples in Different Atmospheres after 7 Years Exposure[a]

	Industrial		Rural		Industrial, Marine	
Couple	W^b	R^c	W	R	W	R
Zn/Zn	187		27		195	
Zn/Fe	332	1.8	81	3.0	349	1.8
Fe/Fe	1825		470		1534	
Fe/Zn	43	1/40	147	1/3	5	1/300

[a]Weight loss of the first metal in a couple (e.g., Zn in Zn/Fe). Samples consisted of two 1.5-in. diameter disks 1/16 in. in thickness, clamped together with 1-in. diameter Bakelite washers, giving an exposed area of 1/16 in. all round the edge of the disk, and an annular area 1/4 in. deep = 1.275 in.^{2}.
[b]See [94]. Weight loss in milligrams.
[c]Corrosion ratio of galvanic couple to nongalvanic couple.

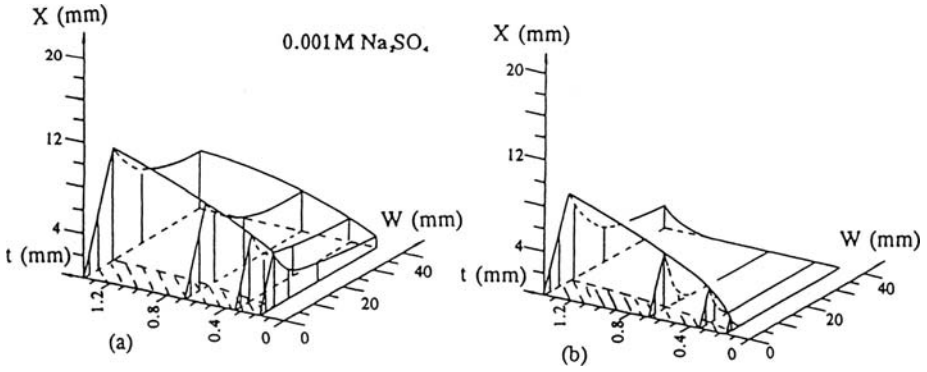

FIGURE 10.6. Protection distance X as function of electrolyte thickness (t), steel width (W), and distance between zinc and steel (D): (a) D = 0; (b) D = 5 mm [87]. (Copyright ASTM. Reprinted with permission.)

series that generally differs from the emf series. Also, as has been discussed earlier, the relative positions of two coupled metals in a galvanic series indicate only the polarity or the flow direction of the galvanic current, but not the magnitude of the current or the rate of corrosion, which is also determined by many other factors. The fundamental relationship in galvanic corrosion is described by Kirchhoff's second law:

$$E_c - E_a = IR_e + IR_m \tag{10.1}$$

where R_e is the resistance of the electrolytic portion of the galvanic circuit, R_m the resistance of the metallic portion, E_c the effective (polarized) potential of the cathodic member of the couple, and E_a the effective (polarized) potential of the anodic member. Generally, R_m is very small and can be neglected. Both E_a and E_c are functions of the galvanic current I; hence, the potential difference between the two metals, when there is a current flow through the electrolyte, does not equal the open-circuit cell potential.

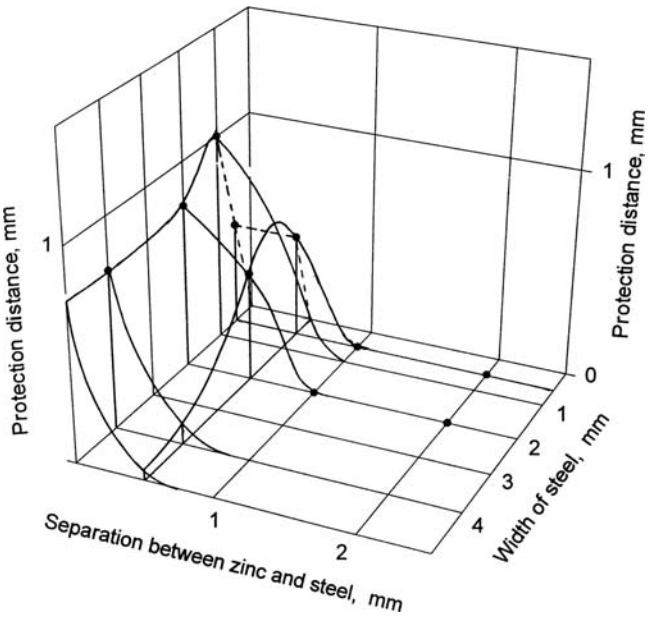

FIGURE 10.7. Protection distance of zinc–steel couple as function of steel width and separation distance under natural atmospheric exposure.

I2. Analysis

Although the mathematical description of galvanic corrosion can be very complex because of the many factors involved, particularly geometric factors, it can be simplified for certain situations. Following is an analysis of coplanar, coupled metals, as illustrated in Figure 10.8(a). Such a geometry applies to a wide range of situations. The distance between anode and cathode (d) may equal zero (e.g., metal joints or a coated metal with the coating partially removed), as shown in Figure 10.8(b). On the other hand, when one metal is used as a sacrificial anode to cathodically protect another metal, the distance between the anode and cathode may be very large, as shown in Figure 10.8(c), that is, $d \gg (x_{ae} - d)$ and $d \gg x_{ce}$ (where $x_{ae} - d$ and x_{ce} are the lengths of anode and cathode, respectively).

The basic current and potential relationships for the geometrical arrangement shown in Figure 10.8(a) can be expressed as follows:

$$I_a = I_c \tag{10.2}$$

and

$$E_{c,corr} - E_{a,corr} = \eta_a(x^a) - \eta_c(x^c) + \Delta V_R(x^a, x^c) \quad \begin{matrix} x^a \le 0 \\ x^c \ge 0 \end{matrix} \tag{10.3}$$

where $E_{a,corr}$ and $E_{c,corr}$ are the uncoupled corrosion potentials of the anode and cathode, respectively; η_a and η_c, the overpotentials of the anode and cathode, respectively, in the couple; and ΔV_R, the ohmic potential drop across the electrolyte between x^a on the anodic surface and x^c on the

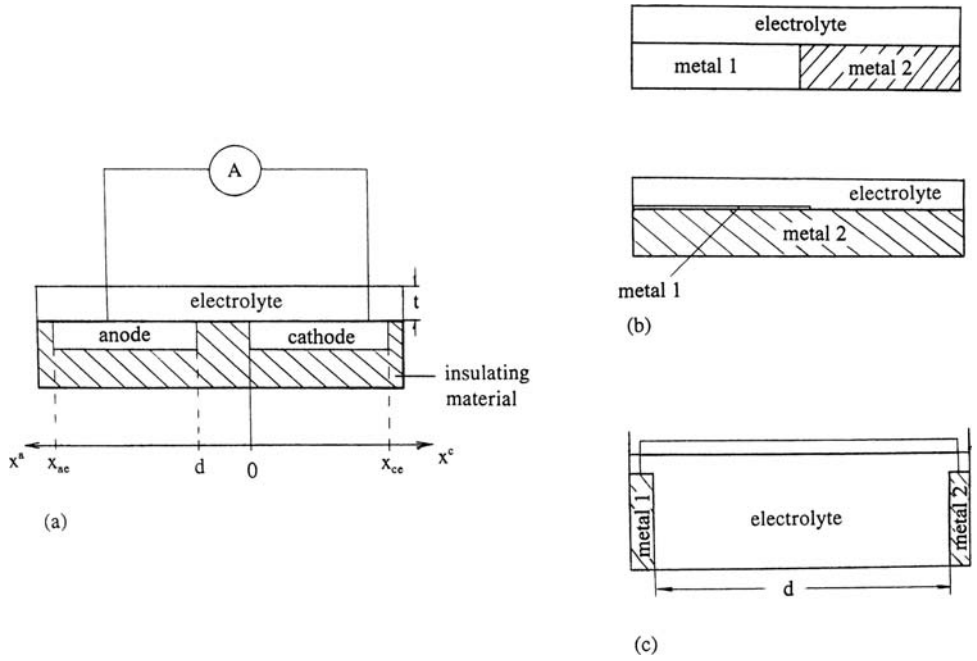

FIGURE 10.8. (a) General geometry of bimetallic couple; (b) bimetallic joint and a metal partially coated with metallic coating; and (c) anode coupled to distant cathode.

cathodic surface; I_a, the total anodic current; and I_c, the total cathodic current. Then,

$$I_a = \int_d^{x_{ae}} i_a(x^a) l \, dx^a \tag{10.4}$$

$$I_c = \int_0^{x_{ce}} i_c(x^c) l \, dx^c \tag{10.5}$$

where l is the width of the electrodes, and $i_a(x^a)$ and $i_c(x^c)$ are the anodic and cathodic current densities, respectively. When both the anodic and cathodic reactions are activation controlled, they can be expressed by the Butler–Volmer equation:

$$I_a = i_{0a}\,\theta_a\{\exp[\beta_{aa}\eta_a(x^a)] - \exp[-\beta_{ac}\eta_a(x^a)]\} \tag{10.6}$$

$$I_c = i_{0c}\,\theta_c\{\exp[\beta_{ac}\eta_c(x^c)] - \exp[-\beta_{cc}\eta_c(x^c)]\} \tag{10.7}$$

where i_{0a} and i_{0c} are the exchange currents for the anodic and cathodic reactions, respectively; β_{aa}, β_{ac}, β_{ca}, and β_{cc}, the kinetic constants; and θ_a and θ_c, the area factors, varying between 0 and 1. Here $\theta = 1$ when the whole surface is fully active and θ is close to zero if the surface is fully passivated. When the cathodic reaction is limited by oxygen diffusion in the electrolyte, Eq. (10.7) is replaced by

$$i_c = 4\mathcal{F}D_O C_{O2}/\delta \tag{10.8}$$

where $\mathcal{F}$ is the Faraday constant; D_O, the diffusion coefficient of oxygen in the electrolyte; C_{O2}, the oxygen concentration in the bulk electrolyte; and δ, the thickness of the diffusion layer.

The total ohmic potential drop in the electrolyte between any two points on the surface of the anode and the cathode for the situation in Figure 10.8(a) consists of three parts:

$$\Delta V_R(x^a, x^c) = \Delta V_a(x^a) + \Delta V_c(x^c) + \Delta V_d \tag{10.9}$$

where ΔV_a, ΔV_c, and ΔV_d represent the ohmic potential drop in the electrolyte in the x direction across the anode, across the cathode, and across the distance between the anode and cathode, respectively. These potential drops can be further expressed by

$$\Delta V_a(x^a) = \int_d^{x^a} j_a(x^a)\, dR(x^a) \tag{10.10}$$

$$\Delta V_c(x^c) = \int_0^{x^c} j_c(x^c)\, dR(x^c) \tag{10.11}$$

$$\Delta V_d = I_a R_d = I_c R_d \tag{10.12}$$

where $R_d = \rho d/tl$, with ρ the resistivity of the electrolyte; t the electrolyte thickness; d the distance between the anode and cathode; l the width of the electrodes; and j_a and j_c the sums of the current from x^a to x_{ae} on the anode and from x^c to

x_{ce} on the cathode, respectively, given by the following Eqs. (10.13) and (10.14):

$$j_a(x^a) = \int_{x^a}^{x_{ae}} i_a(x^a) l \, dx^a \tag{10.13}$$

$$j_c(x^c) = \int_{x^c}^{x_{ce}} i_c(x^c) l \, dx^c \tag{10.14}$$

The factors listed under categories (a)–(f) in Figure 10.1 contribute to galvanic action through the electrochemical reaction kinetics given by Eqs. (10.6) and (10.7). For example, changing the pH of the solution may cause a change of the kinetic parameters, i_{0a}, i_{0c}, β_a, or β_c On the other hand, the geometric factors under category (g) affect galvanic corrosion through the parameters in all the equations from (10.4) to (10.14).

Equations (10.4)–(10.14) describe a general situation. It can be simplified for specific applications and geometry. For example, for Figure 10.8(b), representing the galvanic action of a metal joint or a partially coated metal, the term ΔV_d in Eq. (10.9) becomes zero. For the geometry in Figure 10.8(c), representing galvanic action of two metals separated by a large distance [i.e., $d \gg (x_{ae} - d)$ and $d \gg x_{ce}$], I_a and I_c in Eqs. (10.4) and (10.5) become $i_a A_a$, and $i_c A_c$ with $A_a = l(x_{ae} - d)$ and $A_c = l x_{ce}$, the areas for the anode and the cathode, respectively. In addition, ΔV_a and ΔV_c in Eq. (10.9) can be taken as zero because they are very small compared to ΔV_d. In such a case, the geometry in the galvanic cell (i.e., shape and orientation of electrodes, and size of the electrode) becomes insignificant in the galvanic action of the couple, and the galvanic corrosion of the anode, as well as the galvanic protection of the cathode surface, become uniform. Thus, the galvanic action can be fully described by the polarization characteristics of the anode and the electrolyte resistance without consideration of geometric factors.

I3. Polarization and Resistance

In a galvanic couple, it is important to know the relative contributions from the polarization of the coupled metals and the electrolyte resistance, as described by

$$E_{c,corr} - E_{a,corr} = \Delta V_c + \Delta V_a + IR \tag{10.15}$$

which is essentially Eq. (10.3) simplified when geometric factors are not considered.

Equation (10.15) can be graphically illustrated by the anodic and cathodic polarization curves shown in Figure (10.9). When the solution resistance, R, is infinite, no current flows, and $E_c - E_a$ equals the difference in corrosion potentials of the separated (not coupled) metals (i.e., $E_{c,corr} - E_{a,corr}$). As R decreases, I increases and $E_c - E_a$ becomes smaller because of polarization. When R

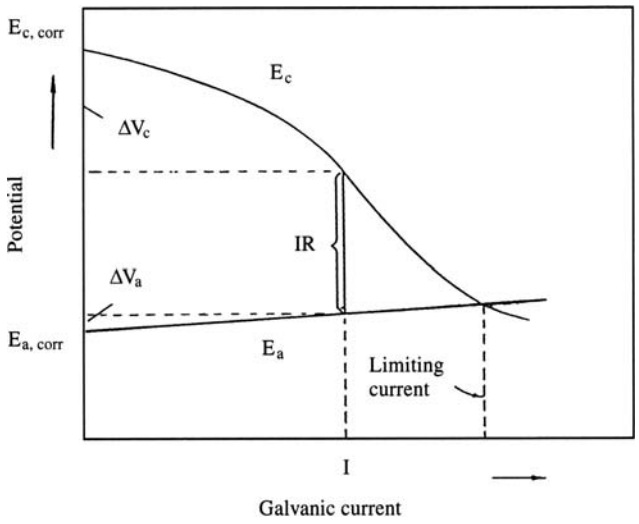

FIGURE 10.9. Graphic estimation of galvanic current.

is zero, $E_c - E_a$, becomes zero and the galvanic current reaches the maximum, known as the "limiting galvanic current," which is at the intersection of the polarization curves of the anode and cathode. The exact shapes of the anodic and cathodic polarization curves depend on the electrochemical reaction kinetics of each metal in the electrolyte and, thus, are functions of pH, temperature, solution concentration, diffusion, formation of passive films, and so on. Often, the anodic dissolution of a nonpassivated metal is activation controlled with a relatively small Tafel slope, while the cathodic reactions on the other metal surface, on the other hand, can either be activation or diffusion controlled depending on the conditions, particularly solution pH and aeration conditions.

The controlling mechanisms in a galvanic corrosion system depend on the relative extent of the anodic and cathodic polarization, on the potential drop in the solution, and on the total potential difference between the coupled metals. If the anode does not polarize and the cathode does, then, in solutions of low resistivity, the current flow is controlled entirely by the cathode. Such a situation is considered to be under cathodic control [Fig. 10.10(a)]. If the anode polarizes and the cathode does not, the status is reversed and the system is said to be under anodic control [Fig. 10.10(b)]. If neither electrode polarizes and the current flow is controlled by the resistivity of the path, mostly in the electrolyte, then the system is said to be under resistance control [Fig. 10.10(c)]. In most situations, a galvanic system is under mixed control, by anodic and cathodic polarization and electrolyte resistance [Fig. 10.10(d)].

The relative magnitude of polarization resistance and solution resistance determines the effective dimension of a galvanic cell, which can be estimated using the polarization parameter, L_i:

$$L_i = 1/\rho |d\eta_i / dI_i| \tag{10.16}$$

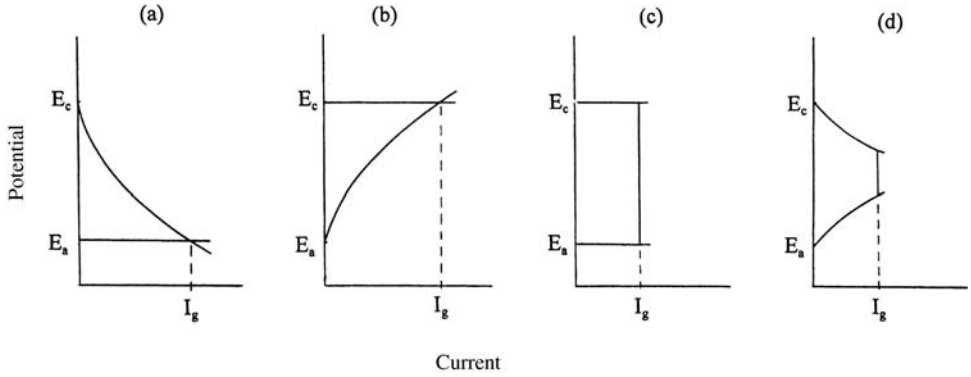

FIGURE 10.10. Schematic illustration of anodic and cathodic polarization carves for four different controlling modes: (a) cathodic control, (b) anodic control, (c) resistance control, and (d) mixed control.

where ρ is the specific resistivity of the electrolyte; I_i is the current density, and η_i is the overpotential of the anode or the cathode. The polarization parameter, defined by Wagner [98], has the dimension of length and provides an electrochemical yardstick for classifying electrochemical systems. It has been widely used to describe the behavior of galvanic corrosion cells [99–102]. Whether the anode and cathode behave "microscopically" or "macroscopically" is determined by the ratio of the dimension of either electrode C_i, divided by the polarization parameter L_i [100]. Mathematical modeling has indicated that, when the ratio, C_i/L_i, is small, the variation of current density across an electrode is small (i.e., the electrode behaves microscopically), On the other hand, when the characterizing ratio is large (i.e., when the electrode dimension is much larger than L_i), the electrode process can be regarded as macroscopic, and the variation of current density across the electrode surface is large.

I4. Potential and Current Distributions

The galvanic action between two metals is governed essentially by the potential distribution across the surface of each electrode. The galvanic current distribution can be determined from the potential distribution when the potential–current relationships for the electrodes are known. Potential distribution can be calculated theoretically or determined experimentally.

Theoretically, a complete description of the potential distribution on the surfaces of a galvanic couple can be obtained by solving Laplace's equation:

$$\nabla^2 E(x, y, z) = 0 \tag{10.17}$$

This equation is derived from Ohm's law, which states that, at any point in the electrolyte, the current density is proportional to the potential gradient

$$I = \sigma \nabla E \tag{10.18}$$

and from the electroneutrality law, which states that, at any point in the electrolyte, the net current under the steady state must be zero

$$\nabla I = 0 \tag{10.19}$$

Many numerical models, with varying mathematical methods and in geometrical and polarization boundary conditions, have been developed for different galvanic systems, as listed in Table 10.9.

These numerical models provide many useful insights to galvanic corrosion. As an example, McCafferty [111] modeled the potential distribution of a concentric circular galvanic corrosion cell, assuming a linear polarization for both the anodic and the cathodic reactions. Figures 10.11 and 10.12 show the results of the potential distribution and current distribution, respectively, as a function of electrolyte thickness. In the bulk electrolyte, the potential variation across the electrodes is small, but both the anode and the cathode are strongly polarized; thus, the actual electrode potentials are far away from E_a^0 and E_c^0. Under a thin-layer electrolyte, the potential variation is large from the anode to the cathode, but both the anode and cathode are only slightly polarized, except for the areas near the boundary between the anode and the cathode. The galvanic current increases with increasing electrolyte thickness. Also, the current is distributed on the electrode surface more uniformly in bulk solutions than in thin-layer solutions where the current is more concentrated near the contact line in the thin electrolyte. According to the calculations of Doig and Flewitt [55], the potential distribution is uniform in the thickness direction under a thin layer of electrolyte (e.g., 1 mm), whereas it is nonuniform under a thick layer of electrolyte. Similar results were reported by Morris and Smyrl [114] for a galvanic cell with coplanar electrodes. The potential distribution under more general geometrical conditions has also been modeled [99, 105].

The results of numerical modeling can be used to predict the galvanic action for the entire surface area of coupled

TABLE 10.9. Studies of Mathematical Modeling for Various Galvanic Systems

Galvanic Couple	Solution	Geometry	Focus	Reference
Cu, Ti, Ni alloys/Zn	Seawater	Cylindrical	Seawater systems	103
Steel/I-600	EDTA solution[a]	Various	Numerical models	104
Fe/Zn	Seawater	General	Modeling	99
Steel/zinc	Seawater	General	Modeling	105
Fe/Cu	0.6 *M* NaCl	Circular disk	Local current	106
S. steel/steel	Water	Coplanar and tubular	Simulation	107
Miscellaneous	Seawater	Tube/sheet	Heat exchanger	23
Carbon/Co	Generic	Sandwich structure	Defects in films	108
Miscellaneous	Seawater	Cylindrical	Heat exchanger	109
Generic	Generic	Random distribution	Heterogeneous surface	70
Generic	Generic	General	Numeric method	110
Generic	Generic	Coplanar strips	Size effects	101
Generic	Generic	Annular electrodes	Thin-layer electrolyte	29
Pt/Fe	0.05 *M* NaCl	Circular cells	Polarization parameters	111
Cu/Zn	0.01 *M* HCl	Coplanar electrodes	Finite differ. analysis	112
Fe/Zn	Seawater	General geometries	Boundary conditions	113

[a]Ethylenediaminetetraacetic acid = EDTA.

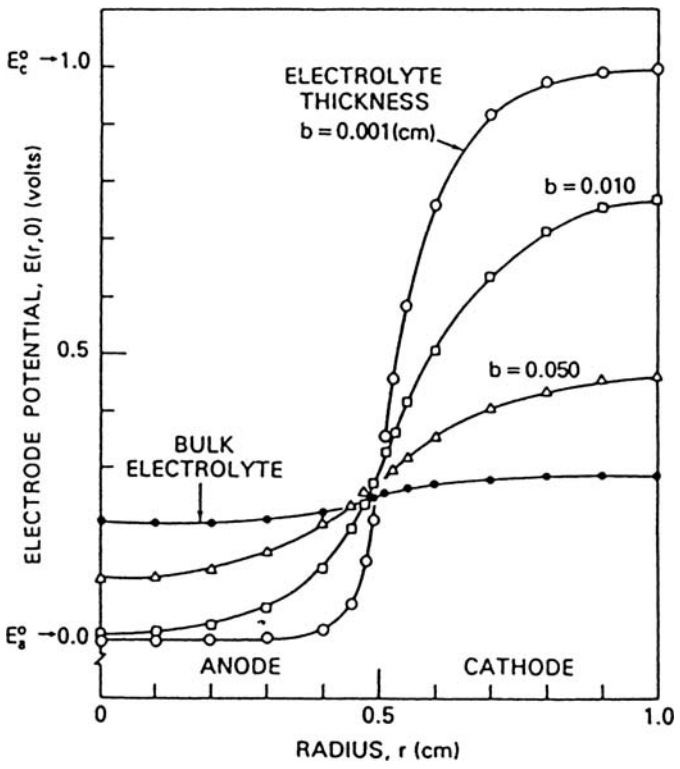

FIGURE 10.11. Distribution of electrode potential for length of anode $L_a = 1$ cm and length of cathode $L_c = 10$ cm for different electrolyte thicknesses. (Anode radius $a = 0.5$ cm, cathode radius $c = 1.0$ cm; $E_0^a = 0$V, $E_0^c = 1$V) [111].

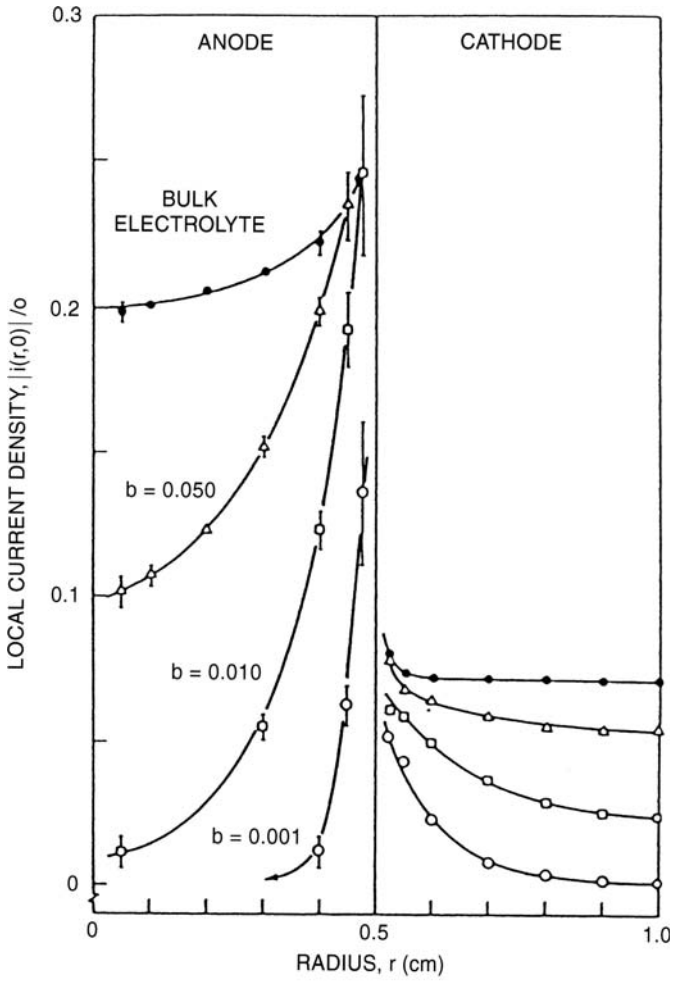

FIGURE 10.12. Current distribution for different electrolyte thicknesses under same conditions as in Figure 10.11 [111].

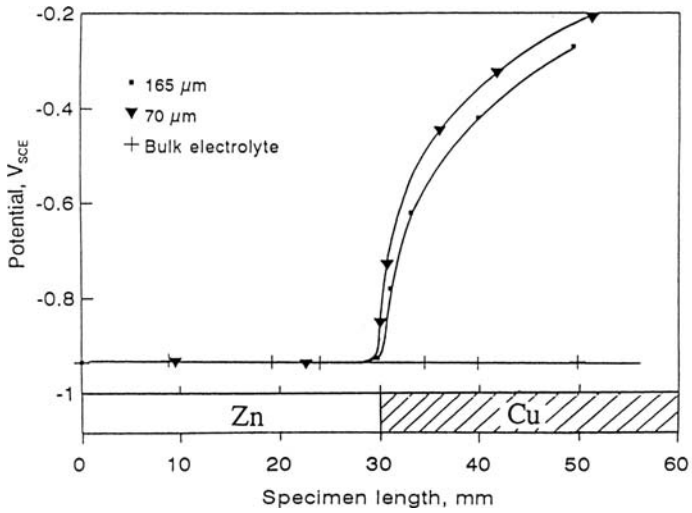

FIGURE 10.13. Distribution of potentials on electrode surface of galvanic couple Cu–Zn in 0.1 *N* NaCl solution as function of electrolyte thickness [54].

metals. For galvanic corrosion in a real structure made of different metals, the boundary conditions must be simplified because it is not possible to include all the conditions experienced by a structure during service, particularly the geometry and the electrode polarization conditions [104, 105, 115]. The geometry of a structure, no matter how complex, is generally fixed for a given situation and is independent of the materials and environmental conditions; the polarization properties of the metals, on the other hand, depend on the interaction of the metals with the environment. The polarization characteristics of a metal electrode are generally different for the anode and for the cathode and they vary in different potential ranges. Sometimes, they also vary with the physical elements in the galvanic system, such as electrolyte thickness [80]. In addition, the electrode properties of the coupled metals usually change with time due to changes on the surfaces and in the solution. These elements must be considered when using a numerical model for predicting long-term behavior is a real galvanic system. More detailed discussion on the advantages and limitations of numerical modeling of galvanic corrosion can be found in the literature [104–106].

The potential distribution on the surface of a galvanic couple can also be experimentally determined by placing a reference electrode close to the metal surface and scanning across the whole surface area of the galvanic couple. Rozenfeld [54] showed that the potential variation on the surface of a coplanar zinc–copper couple greatly increases with decreasing electrolyte thickness on top of the surface, as shown in Figure 10.13. The sharpest potential changes take place on the copper cathode, whereas the anode, except for a very narrow region near the junction, does not polarize. Using this experimental approach, data on potential distribution and galvanic action of the system can be obtained, but this method can be impractical in many situations (e.g., when the structure is so complex that not all the surface area is accessible by a reference electrode).

REFERENCES

1. R. Baboian, G. Haynes, and R. Turcotte, "Galvanic Corrosion on Automobiles," in Galvanic Corrosion, ASTM STP 978, H. P. Hack (Ed.), American Society for Testing and Materials, Philadelphia, PA, 1988, pp. 249–259.
2. V. Kucera and E. Mattsson, "Atmospheric Corrosion of Bimetallic Structures," in Atmospheric Corrosion, W. H. Ailor (Ed.), Wiley, New York, 1982, pp. 561–574.
3. S. W. Dean, "Planning, Instrumentation, and Evaluation of Atmospheric Corrosion Tests and a Review of ASTM Testing," in Atmospheric Corrosion, W. H. Ailor (Ed.), Wiley, New York, 1982, pp. 195–216.
4. C. R. Southwell and J. D. Bultman, "Atmospheric Corrosion Testing in the Tropics," in Atmospheric Corrosion, W. H. Ailor (Ed.), Wiley, New York, 1982, p. 967.
5. T. Fukushima, N. Sato, Y. Hisamatsu, T. Matsushima, and Y. Aoyama, "Atmospheric Corrosion Testing in Japan," in Atmospheric Corrosion, W. H. Ailor (Ed.), Wiley, New York, 1982, pp. 841–872.
6. D. R. Lenard and J. G. Moores, Corros. Sci., **34**, 871 (1993).
7. G. Haynes and R. Baboian, "Atmospheric Corrosion of Clad Metals," in Degradation of Metals in the Atmosphere, ASTM STP 965, S. W. Dean and T. S. Lee (Eds.), American Society for Testing and Materials, Philadelphia, PA, 1988, pp. 145–190.
8. V. Brusic, M. Russak, R. Schad, G. Frankel, A. Selius, D. DiMilia, and D. Edmonson, "Corrosion of Thin Film Magnetic Disc: Galvanic Effects of the Carbon Overcoat," J. Electrochem. Soc., **136**, 42 (1989).

9. A. M. Shams El Din and L. Wang, Br. Corros. J., **28**(4), 271 (1994).
10. G. K. Glass and V. Ashworth, Corros. Sci., **25**(11), 971 (1985).
11. R. B. Hoxeng and C. F. Prutton, Corrosion, **5**(10), 330 (1949).
12. P. T. Gilbert, "An Investigation into the Corrosion of Zinc and Zinc-Coated Steel in Hot Waters," Sheet Metal Industries, Oct.–Dec., 1948.
13. H. L. Shuldener and L. Lehrmen, Corrosion, **14**(12), 17 (1958).
14. C. R. Southwell, J. D. Bultman, and A.L. Alexander, Mater. Perform., **15**(7), 9 (1976).
15. D. R. Gabe and A. M. El Hassan, Br. Corros. J., **21**(3), 185 (1986).
16. S. G. Al Zaharani, B. Todd, and J. W. Oldfield, "Bimetallic Joints in Multistage Flash Desalination Plants," in Galvanic Corrosion, ASTM STP 978, H. P. Hack, (Ed.), American Society for Testing and Materials, Philadelphia, PA, 1988, pp. 323–335.
17. G. A. Gehring, Jr., "Galvanic Corrosion in Power Plant Condensers," in Galvanic Corrosion, ASTM STP 978, H. P. Hack (Ed.), American Society for Testing and Materials, Philadelphia, PA, 1988, pp. 301–309.
18. R. Baboian and G. Haynes, "Galvanic Corrosion of Ferritic Stainless Steels in Seawater," in Corrosion in Natural Environments, ASTM STP 558, W. H. Ailor, S. W. Dean, and F. H. Haynie (Eds.), American Society for Testing and Materials, Philadelphia, PA, 1974, pp. 171–184.
19. S. Schuldiner and R. E. White, J. Electrochem. Soc., **97**(12), 433 (1950).
20. H. P. Hack, "Galvanic Corrosion of Piping and Fitting Alloys in Sulfide-Modified Seawater," in Galvanic Corrosion, ASTM STP 978, H. P, Hack (Ed.), American Society for Testing and Materials, Philadelphia, PA, 1988, pp. 339–351.
21. K. D. Efird, "Galvanic Corrosion in Oil and Gas Production," in Galvanic Corrosion, ASTM STP 978, H. P. Hack (Ed.). American Society for Testing and Materials, Philadelphia, PA, 1988, pp. 260–282.
22. L. S. Redmerski, J. J. Eckenrod, K. E. Pinnow, and W. Kovach, "Experience with Cathodic Protection of Power Plant Condensers Operating with High Performance Ferritic Stainless Steel Tubing," in Galvanic Corrosion, ASTM STP 978, H. P. Hack (Ed.), American Society for Testing and Materials, Philadelphia, PA, 1988, pp. 310–322.
23. J. R. Scully and H. P. Hack, "Prediction of Tube-Tubesheet Galvanic Corrosion Using Finite Element and Wagner Number Analyses," in Galvanic Corrosion, ASTM STP 978, Philadelphia, PA, 1988, pp. 136–157.
24. R. Francis, Br. Corros. J., **29**(1), 53 (1994).
25. H. P. Hack and J. R. Scully, Corrosion, **42**, 79 (1986).
26. R. Foster, H. Hack, and K. Lucas, "Long-Term Current and Potential Data for Selected Galvanic Couples," Paper No. 517, CORROSION/96, NACE, Houston, TX, 1996.
27. M. Romanoff, "Underground Corrosion," Circular 579, U. S. National Bureau of Standards, Washington, DC, 1957.
28. E. Escalante, "The Effect of Soil Resistivity and Soil Temperature on the Corrosion of Galvanically Coupled Metals in Soil," in Galvanic Corrosion, ASTM STP 978, Philadelphia, PA, 1988, pp. 193–202.
29. K. G. Compton, Corrosion, **16**, 87 (1960).
30. N. Sridhar and J. Kolts, "Evaluation and Prediction of Galvanic Corrosion in Oxidizing Solutions," in Galvanic Corrosion, ASTM STP 978, H. P. Hack (Ed.), American Society for Testing and Materials, Philadelphia, PA, 1988, pp. 203–219.
31. R. A. Corbett, W. S. Morrison, and R. Snyder, "Galvanic Corrosion Resistance of Weld Dissimilar Nickel-Base Alloys," in Galvanic Corrosion, ASTM STP 978, H. P. Hack (Ed.), American Society for Testing and Materials, Philadelphia, PA, 1988, pp. 235–245.
32. Y. H. Yau and M. A. Streicher, "Galvanic Corrosion of Duplex Fe–Cr–10%Ni Alloys in Reducing Acids," in Galvanic Corrosion, ASTM STP 978, H. P. Hack (Ed.), American Society for Testing and Materials, Philadelphia, PA, 1988, pp. 220–234.
33. G. O. Davis, J. Kolts, and N. Sridhar, Corrosion, **42**, 329 (1986).
34. E. Symniotis, Corrosion, **46**, 2 (1990).
35. D. A. Jones and A. J. P. Paul, Corrosion, **50**, 516 (1994).
36. W. J. Polock and B. R. Hinton, "Hydrogen Embrittlement of Plated High-Strength 4340 Steel by Galvanic Corrosion," in Galvanic Corrosion, ASTM STP 978, H. P. Hack (Ed.), American Society for Testing and Materials, Philadelphia, PA, 1988, pp. 35–50.
37. L. H. Hihara and P. K. Kondepudi, Corros. Sci., **34**, 1761 (1993).
38. M. J. Pryor and D. S. Keir, J. Electrochem. Soc., **104**(5), 269 (1957).
39. L. M. Wing, J. Commander, J. O'Grady, and T. Koga, "Specifying Zinc Alloy Coatings for Improved Galvanic Corrosion Performance," Paper 971004, SAE, Warrendale, PA, 1997.
40. D. L. Jordan, "Influence of Iron Corrosion Products on the Underfilm Corrosion of Painted Steel and Galvanized Steel," in Zinc-Based Steel Coating Systems: Metallurgy and Performance, G. Krauss and D. K. Matlock (Eds.), TMS, Warrendale, PA, 1990, pp. 195–205.
41. C. Cabrillac and A. Exertier, "The Effect of Coating Composition on the Properties of a Galvanized Coating," in Proceedings of the 7th International Conference on Hot Dip Galvanizing, Paris, Pergamon. New York, June 1964, pp. 289–313.
42. S. Kurokawa, K. Yamato, and T. Ichida, "A Study on Cosmetic and Perforation Corrosion Test Procedures for Automotive Steel Sheets," Paper No. 396, NACE CORROSION'91 Conference, Cincinnati, OH, Mar. 11–15,1991, NACE, Houston, TX, 1991.
43. J. A. von Fraunhofer and A. T. Lubinski, Corros. Sci., **14**, 225 (1974).
44. E. A. Anderson, in Corrosion Resistance of Metals and Alloys, 2nd ed., F. L. LaQue and H. R. Copson (Eds.), Reinhold Publishing, New York, 1963, pp. 223–247.
45. A. Asphahani and H. H. Uhlig, J, Electrochem. Soc., **122**(2), 174 (1975).

46. G. Lauer and F. Mansfeld, Corrosion, **26**(11), 504 (1970).
47. F. Bellucci, Corrosion, **48**(4), 281 (1992).
48. P. Bellucci and G. Capobianco, Br. Corros. J., **24**(3), 219 (1989).
49. F. Bellucci, Corrosion, **47**, 808 (1991).
50. F. Mansfeld and J. V. Kenkel, Corros. Sci., **15**, 239 (1975).
51. F. Mansfeld, D. H. Hengstenberg, and J. V. Kenkel, Corrosion, **30**(10), 343 (1974).
52. L. H. Hihara and R. M. Latanision, Corros. Sci., **34**, 655 (1993).
53. L. H. Hihara and R. M. Latanision, Corrosion, **48**, 546 (1992).
54. I. L. Rozenfeld, Atmospheric Corrosion of Metals, NACE, Houston, TX, 1972.
55. P. Doig and P. E. J. Flewitt, J. Electrochem. Soc., **126**(12), 2057 (1979).
56. A. M. Shams El Din, J. M. Abd El Kader, and M. M. Badran, Br. Corros. J., **16**(1), 32 (1981).
57. S. M. Wilhelm, "Galvanic Corrosion Caused by Corrosion Products," in Galvanic Corrosion, ASTM STP 978, H. P. Hack (Ed), American Society for Testing and Materials, Philadelphia, PA, 1988, pp. 23–34.
58. F. Mansfeld and J.V. Kenkel. Corrosion, **31**, 298 (1974).
59. G. Schick, "Avoiding Galvanic Corrosion Problems in the Telephone Cable Plant," in Galvanic Corrosion, ASTM STP 978, Philadelphia, PA, 1988, pp. 283–290.
60. A. J. Griffin, Jr., S. E. Henandez, F. R. Brotzen, and C. F. Dunn, J. Electrochem. Soc., **141**, 807 (1994).
61. J. Gluszek and J. Masalski, Br. Corros. J., **27**(2), 135 (1992).
62. S. Huang and R. A. Oriani, "The Corrosion Potential of Galvanically Coupled Copper and Zinc Under Humid Gases," Abstract No. 91, Electrochemical Society Extended Abstracts, Fall Meeting, Oct. 10–15, 1993, New Orleans, LA, Electrochemical Society, Pennington, NJ, Vol. 2–93, p. 156, 1993.
63. D. Whiting, D. Stark, and W. Schutt, "Galvanic Anode Cathodic Protection System for Bridge Decks—Updated Results," Paper 41, CORROSION/81, International Corrosion Forum Sponsored by the National Association of Corrosion Engineers, Toronto, ON, Apr. 6–10, 1981.
64. A. Al-Hashem and D. Thomas, "The Effect of Corona Discharge Treatment on the Corrosion Behaviour of Metallic Zinc Spots Contained in Polymeric Coatings," in Proceedings of the International Conference on Zinc and Zinc Alloy Coated Steel Sheet, GALVATECH'89, Tokyo, Japan, Sept. 5–7, 1989, pp. 611–618.
65. X. Sun and S. Tsujikawa, Corros. Eng. (Jpn), **41**, 741 (1992).
66. J. W. Jang, I. Iwasaki, and J. J. Moore, Corrosion, **45**, 402 (1989).
67. S. M. Wilhelm, Corrosion, **48**, 691 (1992).
68. X. G. Zhang and J. Hwang, Mater. Perform., **36**(2), 22 (Feb. 1997).
69. X. G. Zhang, J. Electrochem. Soc., **143**, 1472 (1996).
70. R. Morris and W. Smyrl, J. Electrochem. Soc., **136**, 3237 (1989).
71. S. R. Morrison, Electrochemistry at Semiconductor and Oxidized Metal Electrodes, Plenum, New York, 1980.
72. M. Stratmann and J. Müller, Corros. Sci., **36**(2), 327 (1994).
73. D. L. Jordan, "Galvanic Interactions between Corrosion Products and Their Bare Metal Precursors: A Contribution to the Theory of Underfilm Corrosion," in Proceedings of the Symposium on Advances in Corrosion Protection by Organic Coatings, Vol. B9-3, Electrochemical Society, Pennington, NJ, 1989, pp. 30–43.
74. A. M. Shams El Din, J. M. Abd El Kader, and A. T. Kuhn, Br. Corros. J., **15**(4), 208 (1980).
75. X. G. Zhang, Corrosion and Electrochemistry of Zinc, Plenum, New York, 1996.
76. L. Kenworthy, J. Inst. Metals, **69**, 67 (1943).
77. D. Massinon and D. Thierry, "Rate Controlling Factors in the Cosmetic Corrosion of Coated Steels," Paper No. 574, NACE CORROSION'91 Conference, Mar. 11–15, NACE, Houston, TX, 1991.
78. D. Massinon and D. Dauchelle, "Recent Progress Towards the Understanding of Underfilm Corrosion of Coaled Steels Used in the Automotive Industry," in Proceedings of the International Conference on Zinc and Zinc Alloy Coated Steel Sheet, GALVATECH'89, Tokyo, Japan, Sept. 5–7 1989, pp. 585–595.
79. M. J. Pryor and D. S. Keir, J. Electrochem, Soc., **105**(11), 629 (1958).
80. X. G. Zhang and E. M. Valeriote, Corros. Sci., **34**, 1957 (1993).
81. I. L. Rosenfeld, "Atmospheric Corrosion of Metals. Some Questions of Theory," The 1st International Congress on Metallic Corrosion, London, UK, Apr. 1961, pp. 243–253.
82. D. P. Doyle and T. E. Wright, "Quantitative Assessment of Atmospheric Galvanic Corrosion," in Galvanic Corrosion, ASTM STP 978, American Society for Testing and Materials, Philadelphia, PA, 1988, pp. 161–171.
83. K. G. Compton and A. Mendizza, "Galvanic Couple Corrosion Studies by Means of the Threaded Bolt and Wire Test," ASTM 58th Annual Meeting, Symposium on Atmospheric Corrosion of Non-Ferrous Metals, American Society for Testing and Materials, ASTM STP 175, Philadelphia, PA, 1955, pp. 116–125.
84. A. K. Dey, A. K. Sinha Mahapatra, D. K. Khan, A. N. Mukherjee, R. Narain, K. P. Mukherjee, and T. Banerjee, NML Tech. J. India, **8**(4), 11 (1966).
85. M. E. Warwick and W. B. Hampshire, "Atmospheric Corrosion of Tin and Tin Alloys," in Atmospheric Corrosion, W. H. Ailor (Ed.), Wiley, New York, 1982, pp. 509–527.
86. X. G. Zhang, "Galvanic Protection Distance of Zinc Coated Steels Under Various Environmental Conditions," Paper No. 747, CORROSION/98, NACE, Houston, TX. 1998.
87. X. G. Zhang and E. M. Valeriote, "Galvanic Protection of Steel by Zinc Under Thin Layer Electrolytes," in Atmospheric Corrosion, ASTM STP 1239, W. W. Kirk and H. H. Lawson (Eds.), American Society for Testing and Materials, Philadelphia, PA, 1995, pp. 230–239.
88. M. G. Fontana and N. D. Greene, Corrosion Engineering, 2nd ed., McGraw-Hill, New York, 1978, p. 32.
89. F. Mansfeld and J. V. Kenkel, Corrosion, **33**(7), 236 (1977).

90. F. Mansfeld and J. V. Kenkel, Corrosion, **31**(8), 298 (1975).
91. G. Schikorr, Trans. Electrochem. Soc., **76**, 247 (1939).
92. R. B. Hoxeng, Corrosion, **6**(9), 308 (1950).
93. A. G. S. Morton, "Galvanic Corrosion in Navy Ships," in Galvanic Corrosion, ASTM STP 978, H. P. Hack (Ed.), American Society for Testing and Materials, Philadelphia, PA, 1988, pp. 291–300.
94. H. P. Hack, Galvanic Corrosion Test Methods, NACE International, Houston, TX, 1993.
95. L. Sherwood, "Sacrificial Anodes," in Corrosion, vol. 2, L. L. Shreier, R. A. Jarman, and G. T. Burstein (Eds.), Butterworth Heinemann, 1995, pp. 1029–1054.
96. T. J. Lennox, Jr., "Electrochemical Properties of Mg, Zn and Al Galvanic Anodes in Sea Water," Proceedings of the Third International Congress on Marine Corrosion and Fouling, Gaithersburg, MD, Oct. 2–6, 1972, National Technical Information Service (NTIS), Alexandria, VA, 1974, pp. 176–190.
97. D. Massinon, D. Dauchelle, and J. C. Charbonnier, Mater. Sci. Forum, **44–45**, 461 (1989).
98. C. Wagner, J. Electrochem. Soc., **99**(1), 1 (1952).
99. R. S. Munn and O. F. Devereux, Corrosion, **47**(8), 618 (1991).
100. S. M. Abd El Haleem, Br. Corros. J., **11**(4), 215 (1976).
101. J. T. Waber, "Analysis of Size Effects in Corrosion Processes," in Localized Corrosion, NACE, Houston, TX, 1974, pp. 221–237.
102. J. T. Waber et al., J. Electrochem. Soc., **101**(6), 271 (1954); **102**(6), 344 (1955); **102**(7), 420 (1955); **103**(1), 64 (1956); **103**(2), 138 (1956); **103**(10), 567 (1956).
103. D. J. Astlry, "Use of the Microcomputer for Calculation of the Distribution of Galvanic Corrosion and Cathodic Protection in Seawater Systems," in Galvanic Corrosion, ASTM STP 978, H. P. Hack (Ed.), American Society for Testing and Materials, Philadelphia, PA, 1988, pp. 53–78.
104. J. W. Fu, "Galvanic Corrosion Prediction and Experiments Assisted by Numerical Analysis," in Galvanic Corrosion, ASTM STP 978, H. P. Hack (Ed.), American Society for Testing and Materials, Philadelphia, PA, 1988, pp. 79–85.
105. R. A. Adey and S. M. Niku, "Computer Modelling of Galvanic Corrosion," in Galvanic Corrosion, ASTM STP 978, H. P. Hack (Ed.), American Society for Testing and Materials, Philadelphia, PA, 1988, pp. 96–117.
106. R. G. Kasper and C. R. Crowe, "Comparison of Localized Ionic Currents as Measured From 1-D and 3-D Vibrating Probes with Finite-Element Predictions for an Iron-Copper Galvanic Couple," in Galvanic Corrosion, ASTM STP 978, H. P. Hack (Ed.), American Society for Testing and Materials, Philadelphia, PA, 1988, pp. 118–135.
107. E. Bardal, R. Johnsen, and P. O. Gartland, Corrosion, **40**, 628 (1984).
108. A. Kassimati and W. H. Smyrl, J. Electrochem. Soc., **136**, 2158 (1989).
109. D. J. Astley and J. C. Bowlands, Br. Corros. J., **20**(2), 90 (1985).
110. R. B. Morris, J. Electrochem. Soc., **137**, 3039 (1990).
111. E. McCafferty, J. Electrochem. Soc., **124**(12), 1869 (1977).
112. P. Doig and P. E. J. Flewitt, Br. Corros. J., **13**(3), 118 (1978).
113. R. S. Munn and O. F. Devereux. Corrosion, **47**(8), 612 (1991).
114. R. Morris and W. Smyrl, J. Electrochem. Soc., **136**(11), 3229 (1989).
115. F. LaQue, Corrosion, **39**, 36 (1983).